A NEW DESALINATION OF SALINE WATER WITH LANTHANUM ORGANIC FRAMEWORKS

A. Mao-Long Chen[1], B. Si-Yuan Wang[2], and C. Zhao-Hui Zhou[3]*

[1] *State Key Laboratory for Physical Chemistry of Solid Surfaces and College of Chemistry and Chemical Engineering, Xiamen University; College of Chemistry and Biological Engineering, Changsha University of Science & Technology, E-mail: cust_mlchen@126.com*
[2] *State Key Laboratory for Physical Chemistry of Solid Surfaces and College of Chemistry and Chemical Engineering, Xiamen University, E-mail: 762747808@qq.com*
[3] *State Key Laboratory for Physical Chemistry of Solid Surfaces and College of Chemistry and Chemical Engineering, Xiamen University, E-mail: zhzhou@xmu.edu.cn*

ABSTRACT

Lanthanum organic frameworks $\{La(H_2O)_4[La(1,3\text{-}pdta)(H_2O)]_3\}_n \cdot XnH_2O \cdot YnEtOH$ [X = 12, Y = 0 **1**; X = 3, Y = 0 **1a**; X = 0, Y = 0 **1b**; X = 3, Y = 3 **1c**; $1,3\text{-}H_4pdta = CH_2[CH_2N(CH_2CO_2H)_2]_2$] have been isolated from the reactions of lanthanum chloride and 1,3-propanediaminetetraacetate with unusual solvent transport properties for low-pressure desalination. $\{La(H_2O)_4[La(1,3\text{-}pdta)(H_2O)]_3\}_n \cdot 12nH_2O$ (**1**) could be converted reversibly to its trihydrates $\{La(H_2O)_4[La(1,3\text{-}pdta)(H_2O)]_3\}_n \cdot 3nH_2O$ (**1a**), dehydrated product $\{La(H_2O)_4[La(1,3\text{-}pdta)(H_2O)]_3\}_n$ (**1b**) and ethanol adduct $\{La(H_2O)_4[La(1,3\text{-}pdta)(H_2O)]_3\}_n \cdot 3nH_2O \cdot 3nEtOH$ (**1c**). The regular hexagonal **1** with 10.0 Å hydrophobic open-channels containing water nanotubes (WNTs, Φ = 4.2 Å) can be used directly for a very small-scale saline water desalination under room temperature, which show low energy consumption and environmentally friendly process. The nano-confined WNTs can be removed at a low temperature (45 °C). The nano-confined ethanol in **1c** shows a remarkable downfield shift ($\Delta\delta$ = 6.0 ppm) for methylene group in solid state ^{13}C NMR spectrum compared with that of free EtOH.

Keywords: Lanthanum, MOFs, Desalination, Saline water, 1,3-propanediaminetetraacetate

1   INTRODUCTION

The ocean area accounts for 71% of the earth's surface area, resulting in 98% of the water being saline water. The depletion of freshwater resources has attracted more and more attentions. Seawater desalination offers a convenient and inexhaustible source of fresh water from the ocean. Among the current desalination technologies, relatively mature distillation, electrodialysis, and reverse osmosis have been widely used throughout the world. Since seawater desalination is an energy intensive technology, the potential environmental impacts of large-scale seawater desalination plants are also a huge test (Shannon *et al.*, 2008, Elimelech and Phillip, 2011). The reverse osmosis (RO) method has attracted the attention of scholars because of its low energy consumption and environmental protection (Qasim *et al.*, 2019, Ali *et al.*, 2019). Reverse osmosis is a membrane separation process which leads to the desalination market for saline water desalination (Greenlee *et al.*, 2009, Lee, Arnot and Mattia, 2011). Metal-organic framework (MOF) materials show state-of-art applications in many fields such as gas adsorption and separation (Horike *et al.*, 2012, McDonald *et al.*, 2011), chemical sensors (Kreno *et al.*, 2012, Qiu *et al.*, 2019), catalysts (Xiao and Jiang, 2019, Dhakshinamoorthy,Asiri and Garcia, 2019, Drout, Robison and Farha, 2019), magnetic and luminescent materials (Rocha *et al.*, 2011, Kurmoo, 2009, Cui *et al.*, 2012) and desalination (Chen *et al.*, 2014). MOFs used to desalinate saline water will be a novel application.

Here, lanthanum 1,3-propanediaminetetraacetate $\{La(H_2O)_4[La(1,3\text{-}pdta)(H_2O)]_3\}_n \cdot 12nH_2O$ (**1**), its dehydrated   products $\{La(H_2O)_4[La(1,3\text{-}pdta)(H_2O)]_3\}_n \cdot 3nH_2O$ (**1a**)   and $\{La(H_2O)_4[La(1,3\text{-}$

pdta)(H$_2$O)]$_3$}$_n$ (**1b**), and ethanol product {La(H$_2$O)$_4$[La(1,3-pdta)(H$_2$O)]$_3$}$_n$·3nH$_2$O·3nEtOH (**1c**) with MOF structure have been obtained, which are used to desalinate the saline water directly.

2   RESULTS AND DISCUSSIONS

2.1   Crystal Structures

In **1**, each 1,3-pdta chelates one lanthanum ion (La1) by two nitrogen atoms and four carboxyl groups. One of the four carboxyl groups of 1,3-pdta not only chelates La1 but also chelates La2. In this way, the center La2 is connected to the three surrounding La1-pdta units. Two of the carboxy groups and two lanthanum ion (La1 and La2) form two four-membered rings. Twelve La1 ions and six La2 ions form an eighteen-membered lanthanum ring as shown in Figure 1, in which the diameter of the center channel is 10.0 Å. Since La1 is shared by two rings and La2 by three rings, the ratio of La1: La2 is 3: 1.
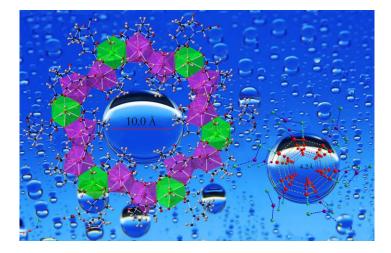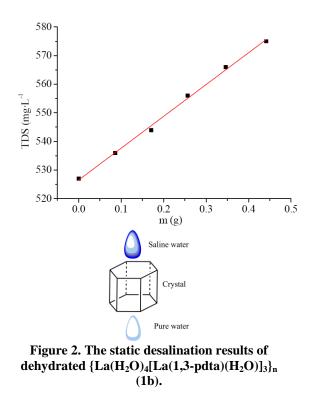

Figure 1. Diagram of eighteen-membered lanthanum ring which shows the central methylene groups in 1,3-pdta ligand toward the center of channel and water molecules in the open-channel of complex {La(H$_2$O)$_4$[La(1,3-pdta)(H$_2$O)]$_3$}$_n$·12nH$_2$O (1) viewed down *c* direction of WNTs and the contact with the open-channel and shows a 4.2 Å nanotube.

It is worth noting that there are water nanotubes (WNTs, Φ = 4.2 Å) lodged in the open-channel (10.0 Å) which is similar to but bigger than that in the former report (Unruh *et al.*, 2013). The distances of hydrogen bonds between the oxygen atoms of water molecules and the carboxy oxygen of the surrounded 1,3-pdta are 2.629, 2.667 and 2.677 Å respectively. Strong hydrogen bonds stabilize water nanotubes. When **1** was heating at 50 °C or immersed in ethanol for one hour, the WNTs were removed to obtaining its trihydrates **1a**. After **1** or **1a** is heated at 120 °C for one hour, all guest water molecules depart from the channels to giving **1c**. When immersed in ethanol for one week or longer time, ethanol molecules replaced water molecules and filled the channels to giving **1c**. The hydrogen bonds distances between the oxygen atoms of ethanol molecules and the carboxy oxygen are 2.771−3.063 Å. The hydrogen bonds are weaker than those in **1** and **1a**.

2.2   Desalination of Sea Water

In contrast to the membrane separation with concentration gradients (Greenlee *et al.*, 2009, Lee,Arnot and Mattia, 2011, Fritzmann *et al.*, 2007, Zhao *et al.*, 2012), **1b** can be exploited to desalinate saline water. Water molecules can pass directly through the channels of **1b**, but salt ions cannot pass through the channels. The total dissolved solid (TDS) of the solution increases linearly with the increments of **1b** as shown in Figure 2. Further, rigorous dynamic desalination experiments with new hexagonal prism crystals and small Perspex partition were carried out with a micro flow rate of 1.1 g water per h at 40°C. The TDS value decrease from 527 mg/L to 0 mg/L at 0.12 Mpa.
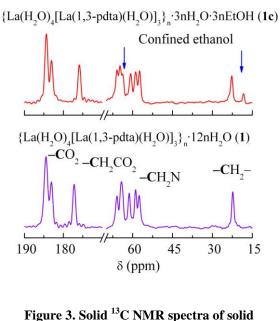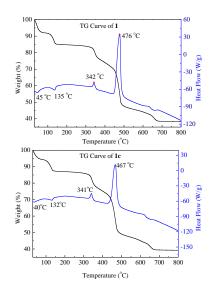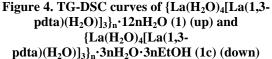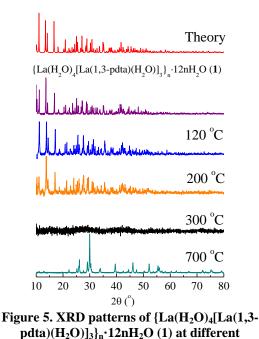
Figure 2. The static desalination results of dehydrated {La(H$_2$O)$_4$[La(1,3-pdta)(H$_2$O)]$_3$}$_n$ (1b).

Figure 3. Solid ^{13}C NMR spectra of solid {La(H$_2$O)$_4$[La(1,3-pdta)(H$_2$O)]$_3$}$_n$·12nH$_2$O (1) and {La(H$_2$O)$_4$[La(1,3-pdta)(H$_2$O)]$_3$}$_n$·3nH$_2$O·3nEtOH (1c).

2.3   Solid State ^{13}C NMR Spectra

The solid state ^{13}C NMR spectra of **1** and **1c** are shown in Figure 3 and Table S4. Three set of ^{13}C NMR signals at 184.5, 183.1 and 177.2 ppm for carboxy groups can be ascribed to the three types of coordination modes of carboxy groups, showing downfield shifts compared with those of free 1,3-pdta (β-CO$_2$ 178.5 ppm). In **1c** and **1**, the chemical shift of a carboxy group shows an obvious highfield shift from 177.2 to 175.9 ppm, supporting the interaction between hydroxyl group of ethanol and carboxy group. Two new peaks at 63.8 and 18.3 ppm can be ascribed to methylene and methyl groups of ethanol. The methylene group shows downfield shift (Δδ = 6.0 ppm) comparing with solution ethanol due to the nano-effects in the channels.

Figure 4. TG-DSC curves of {La(H$_2$O)$_4$[La(1,3-pdta)(H$_2$O)]$_3$}$_n$·12nH$_2$O (1) (up) and {La(H$_2$O)$_4$[La(1,3-pdta)(H$_2$O)]$_3$}$_n$·3nH$_2$O·3nEtOH (1c) (down)

Figure 5. XRD patterns of {La(H$_2$O)$_4$[La(1,3-pdta)(H$_2$O)]$_3$}$_n$·12nH$_2$O (1) at different temperatures.

3

2.4   Thermogravimetric Analysis and X-ray Diffraction Patterns

The thermal stability and decomposition pattern of **1** in Figure 4 show the first weight loss of **1** occurring at around 45 °C that correspond to the loss of partial guest water molecules in the hydrophobic channel by protruding methylene groups of 1,3-pdta. The release of remaining guest water molecules were from 115 to 140 °C. The weight of **1** remains stable until around 342 °C. The ligands in **1** decompose step by step and transform into La_2O_3 from 340 to 490 °C. The decomposition pattern of **1c** is similar to that of **1**, but the first weight loss is around 40 °C, indicating the evaporation of ethanol at lower temperature due to nano-effect of the ethanol in confined environment.

Powder X-ray diffraction patterns of **1** in Figure 5 demonstrate a well maintained framework up to 200 °C. At 300 °C, the XRD pattern reveals the collapse of the framework probably owing to the loss of some coordination water molecules.

2.5   IR Spectroscopy and Fluorescence Spectrum

IR spectra for **1**, **1a**, **1b** and **1c** are presented in Figure 6. The bands at 1583 ~ 1579 cm^{-1} and 1455 ~ 1414 cm^{-1} are attributed to asymmetric and symmetric vibrations of carboxy groups of ligands. Compared with free carboxylic acidic group (1740 ~ 1700 cm^{-1}), the absorptions are red shifts due to the coordination of carboxy groups with La(III) ions, which reduces the bond strength of C−O bond. No obvious difference between **1**, **1a**, **1b** and **1c** is observed due to 1,3-pdta ligand with too many methylene groups and the very strong vibrations of carboxy groups.
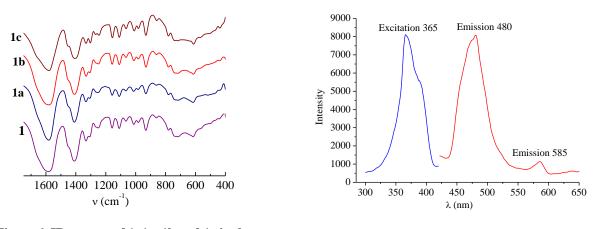

Figure 6. IR spectra of 1, 1a, 1b and 1c in the range from 1750 cm^{-1} to 400 cm^{-1}.

Figure 7. Fluorescence spectrum (Excitation and emission) of 1

The fluorescence spectral properties of **1** in Figure 7 reveal maximum peaks at 365 nm in the excitation spectrum and at 480 and 585 nm in the emission spectrum. The emission spectrum indicates that **1** with rare earth metal can emit visible light. In comparison with metal salt (451 nm), the fluorescence spectra of the complexes show red shift due to the charge transfer of the rare earth ions to the ligand (MLCT).

3   CONCLUSIONS

Lanthanum organic frameworks {La(H$_2$O)$_4$[La(1,3-pdta)(H$_2$O)]$_3$}$_n$·XnH$_2$O·YnEtOH [X = 12, Y = 0 **1**; X = 3, Y = 0 **1a**; X = 0, Y = 0 **1b**; X = 3, Y = 3 **1c**] have been isolated. The guest water molecules in 1 can be programmed to be lost or replaced by ethanol molecules to convert to **1a**, **1b** or **1c**, when **1** was immersing in ethanol or heating at 50 and 120 °C respectively, during which these MOFs kept a robust framework. The application of lanthanum MOF **1b** in saline water desalination has been studied. Although the performance of saline water desalination still needs to be improved for large scale, such a low-energy and environmentally friendly desalination process provides a new method with MOFs.

ACKNOWLEDGMENTS

REFERENCES

Ali, Z. *et al.* (2019) 'Defect-free highly selective polyamide thin-film composite membranes for desalination and boron removal'. *J. Membr. Sci.,* 578 85-94, doi: 10.1016/j.memsci.2019.02.032

Chen, M.L. *et al.* (2014) 'A lanthanum chelate possessing an open-channel framework with water nanotubes: properties and desalination'. *Dalton Trans,* 43 (16), pp. 6026-6031, doi: 10.1039/c3dt52837e

Cui, Y. *et al.* (2012) 'Luminescent functional metal-organic frameworks'. *Chem. Rev.,* 112 (2), pp. 1126-1162, doi: 10.1021/cr200101d

Dhakshinamoorthy, A., Asiri, A.M. and Garcia, H. (2019) 'Formation of C-C and C-heteroatom bonds by C-H activation by metal organic frameworks as catalysts or supports'. *ACS Catal.,* 9 (2), pp. 1081-1102, doi: 10.1021/acscatal.8b04506

Drout, R.J., Robison, L. and Farha, O.K. (2019) 'Catalytic applications of enzymes encapsulated in metal-organic frameworks'. *Coord. Chem. Rev.,* 381 151-160, doi: 10.1016/j.ccr.2018.11.009

Elimelech, M. and Phillip, W.A. (2011) 'The future of seawater desalination: energy, technology, and the environment'. *Science,* 333 (6043), pp. 712-717, doi: 10.1126/science.1200488

Fritzmann, C. *et al.* (2007) 'State-of-the-art of reverse osmosis desalination'. *Desalination,* 216 1-76, doi: 10.1016/j.desal.2006.12.009

Greenlee, L.F. *et al.* (2009) 'Reverse osmosis desalination: water sources, technology, and today's challenges'. *Water research,* 43 (9), pp. 2317-2348, doi: 10.1016/j.watres.2009.03.010

Horike, S. *et al.* (2012) 'A solid solution approach to 2D coordination polymers for CH4/CO2 and CH4/C2H6 gas separation: equilibrium and kinetic studies'. *Chem. Sci.,* 3 (1), pp. 116-120, doi: 10.1039/c1sc00591j

Kreno, L.E. *et al.* (2012) 'Metal-organic framework materials as chemical sensors'. *Chem. Rev.,* 112 (2), pp. 1105-1125, doi: 10.1021/cr200324t

Kurmoo, M. (2009) 'Magnetic metal-organic frameworks'. *Chem. Soc. Rev.,* 38 (5), pp. 1353-1379, doi: 10.1039/b804757j

Lee, K.P., Arnot, T.C. and Mattia, D. (2011) 'A review of reverse osmosis membrane materials for desalination—Development to date and future potential'. *J. Membrane Sci.,* 370 1-22, doi: 10.1016/j.memsci.2010.12.036

McDonald, T.M. *et al.* (2011) 'Enhanced carbon dioxide capture upon incorporation of N,N '-dimethylethylenediamine in the metal-organic framework CuBTTri'. *Chem. Sci.,* 2 (10), pp. 2022-2028, doi: 10.1039/c1sc00354b

Qasim, M. *et al.* (2019) 'Reverse osmosis desalination: A state-of-the-art review'. *Desalination,* 459 59-104, doi: 10.1016/j.desal.2019.02.008

Qiu, Q. *et al.* (2019) 'Recent advances in the rational synthesis and sensing applications of metal-organic framework biocomposites'. *Coord. Chem. Rev.,* 387 60-78, doi: 10.1016/j.ccr.2019.02.009

Rocha, J. *et al.* (2011) 'Luminescent multifunctional lanthanides-based metal-organic frameworks'. *Chem. Soc. Rev.,* 40 (2), pp. 926-940, doi: 10.1039/c0cs00130a

Shannon, M.A. *et al.* (2008) 'Science and technology for water purification in the coming decades'. *Nature,* 452 (7185), pp. 301-310, doi: 10.1038/nature06599

Unruh, D.K. *et al.* (2013) 'Development of metal-organic nanotubes exhibiting low-temperature, reversible exchange of confined "ice channels"'. *J. Am. Chem. Soc.,* 135 (20), pp. 7398-7401, doi: 10.1021/ja400303f

Xiao, J.D. and Jiang, H.L. (2019) 'Metal-organic frameworks for photocatalysis and photothermal catalysis'. *Acc. Chem. Res.,* 52 (2), pp. 356-366, doi: 10.1021/acs.accounts.8b00521

Zhao, S. *et al.* (2012) 'Recent developments in forward osmosis: Opportunities and challenges'. *J. Membrane Sci.,* 396 1-21, doi: 10.1016/j.memsci.2011.12.023